Journal of Magnetism and Magnetic Materials 89 (1990) 167–172
North-Holland

ANNEALING EFFECT ON MAGNETIC PROPERTIES OF Si-MODIFIED γ-Fe_2O_3 PARTICLES

J.H. HSU, C.R. CHANG

Physics Department, National Taiwan University, Taipei, Taiwan

P.C. KUO and J.H. HUANG

The Graduate Institute of Materials Engineering, National Taiwan University, Taipei, Taiwan

Received 28 August 1989; in revised form 13 March 1990

Acicular γ-Fe_2O_3 particles are synthesized by dehydration, reduction and oxidation of acicular γ-FeOOH particles. The annealing treatment has been added preceding the reduction step in the preparation of acicular γ-Fe_2O_3 particles. We studied the annealing effect from the investigation of particle morphology, coercive force as well as magnetization. It has been found that Si adsorption on the surface of the particle will significantly improve the annealing effect. Furthermore, it causes an anomalous increase in the coercive force. The origins of annealing effect and H_c enhancement are discussed.

1. Introduction

The acicular γ-Fe_2O_3 particles have been used as the major recording material over several decades due to its excellent combination of cost and performance [1]. One of the conventional methods to prepare iron oxide particles is as follows:

$$\gamma\text{-(FeO)OH} \xrightarrow{dehydration} \gamma\text{-}Fe_2O_3 \xrightarrow{reduction} Fe_3O_4 \xrightarrow{oxydation} \gamma\text{-}Fe_2O_3.$$

Unfortunately, with this method, the amount of voids or micropores is very high inside these particles which are sources of self-demagnetizing field. But the micropores can be reduced both in number and volume with high temperature heat treatment. As it is well known that the coercive force (H_c) of the γ-Fe_2O_3 is mainly originated from the shape anisotropy [2], good acicular shape has to be preserved during the whole process in order to attain high H_c. The high temperature treatment however will cause the collapse of acicularity and the occurrence of sintering between particles. Therefore, the heating treatments has to be carried out under the adequate conditions. Or some modified method to coat the particles has to be undertaken before heat treatments at high temperatures. A wide range of chemicals has been used [3]. In this paper, we report the results from investigation of silica adsorbed γ-Fe_2O_3 particles with adding the procedure of annealing treatment before the step of reduction. Our data show that improved magnetic properties have been achieved. The possible reasons of increasing coercive force are also discussed analytically.

2. Experimental

The preparation of γ-Fe_2O_3 particles begins with the fabrication of γ-(FeO)OH seeds. $FeCl_2$ solution and NaOH solution with suitable concentrations are mixed together. This aqueous solution is flown into air and stirred at room temperature to precipitate acicular γ-(FeO)OH seeds. These seeds are then used as the nuclei to grow larger acicular particles (length ≈ 0.4 μm).

The coating process is performed at the stage of γ-(FeO)OH. The silica-coated lepidocrocite is obtained by dispersing 10 g γ-(FeO)OH powder into 500 ml distilled water and then adding the proper amount of Na_2SiO_3 into the solution. The PH value of the solution is maintained at 6 and stirred for another hour. The content of Si is determined from atomic absorption analysis.

The reduction of γ-Fe_2O_3 to Fe_3O_4 is carried out in the mixed gases of H_2 and H_2O to prevent from over-reduction to α-Fe. The reduction time is 20 min. The subsequent oxidation step is undertaken at 300 °C for one hour.

The structures of the particles are determined from X-ray diffraction pattern. The crystallite size, t, of the acicular particles can be obtained from the width of the diffraction peak by using the Scherrer formula [4]

$$t = 0.9\lambda / B \cos \theta_B, \qquad (1)$$

where λ is the wavelength of X-ray, B the half width of diffraction peak and θ_B the angle of peak position. The dehydration temperature of γ-(FeO)OH $\rightarrow \gamma$-Fe_2O_3 is determined from thermogravimetric analysis. The heating rate is kept at 5 °C/min. Magnetic measurements are performed on a sample vibrating magnetometer with a maximum applied field of 5 kG.

3. Results and discussion

The dehydration temperature of γ-(FeO)OH particle, T_d, is plotted in fig. 1 as a function of Si content. It is found that T_d is gradually increasing with Si content. During the dehydration process, the following reaction takes place: $2\gamma\text{-(FeO)OH} \rightarrow \gamma\text{-}Fe_2O_3 + H_2O$. The increase of T_d with Si content suggests that Si adsorption inhibits the removal of crystallization water from the particles.

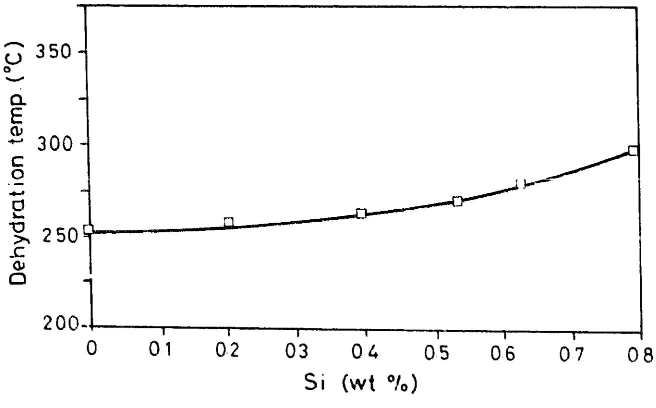

Fig. 1. The dehydration temperature (T_d) of γ-(FeO)OH as a function of Si content.

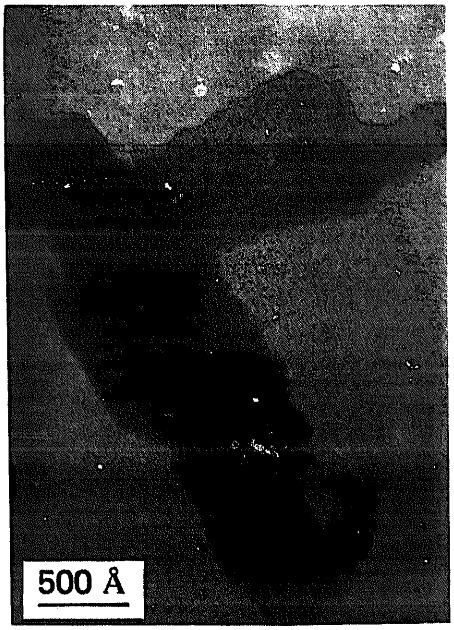

Fig. 2. Micrograph of modified γ-Fe_2O_3 with 0.42 wt% Si after dehydration at 280 °C for 30 min.

The γ-Fe_2O_3 particles which are obtained from the dehydration of γ-(FeO)OH contains many micropores and shows poor magnetic behavior. The TEM micrograph with 0.42 wt% Si is shown in fig. 2. The crystallite size calculated from X-ray diffraction pattern is about 58 Å which is consistent with the estimate from the TEM picture (also see fig. 2).

In fig. 3 it is indicated that the widths of X-ray diffraction peaks becomes narrower as the annealing temperature, T_a, rises. It also indicates that the second phase, α-Fe_2O_3, appears when T_a reaches around 480 °C. The transformation into α-Fe_2O_3 completes at about 550 °C. The crystallite sizes of α-Fe_2O_3 particles as well as of the resultant γ-Fe_2O_3 particles, plotted as a function of T_a, are shown in fig. 4. It points out that the crystallite grows larger with increasing T_a. This result is owing to the intragranular sintering, which reduces the amount of cavity. Meanwhile, the pore is also enhanced and eventually the breakage of crystallites happens if T_a is above 720 °C. This mechanism can be well elucidated by fig. 5.

In fig. 6, H_c versus T_γ, the reduction temperature, are reported for several T_a's. All curves ex-

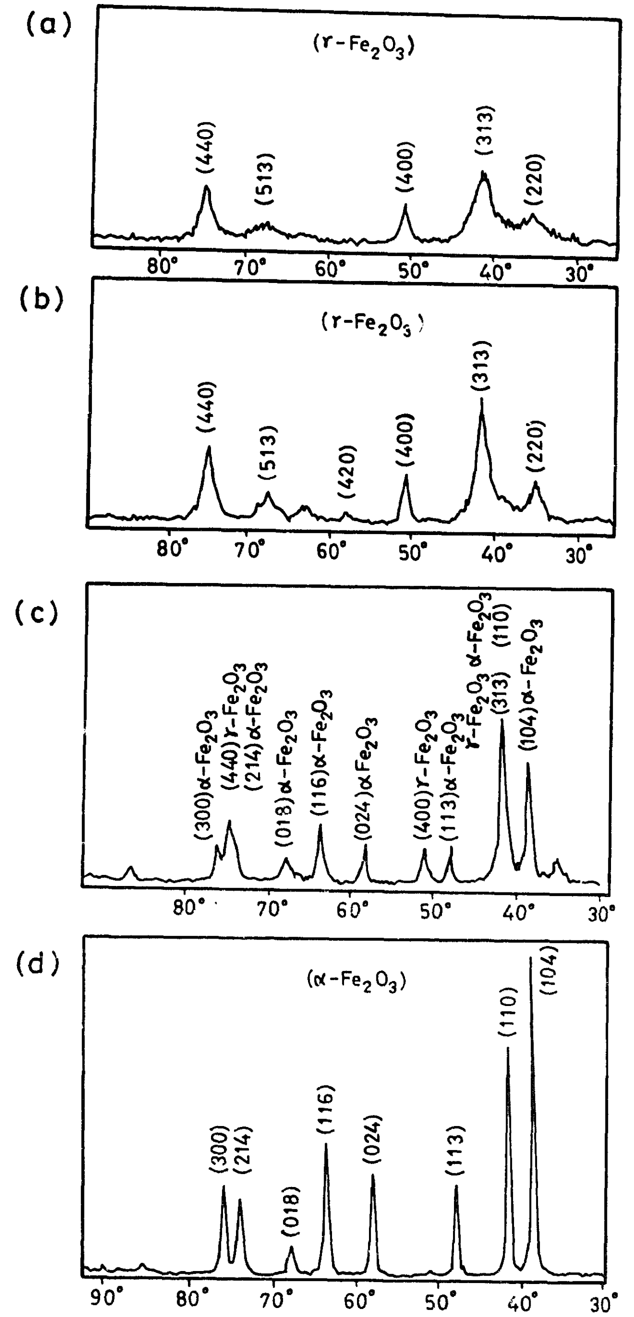

Fig. 3. X-ray diffraction patterns of γ-Fe_2O_3 after annealing. The annealing time is 1 h. (a) $T_a = 280\,°C$. (b) $T_a = 420\,°C$, (c) $T_a = 480\,°C$, (d) $T_a = 550\,°C$.

hibits the trend that H_c initially increases with T_γ and reaches a maximum at T_γ^{max} before it falls abruptly. The increase of H_c is due to the reduction of micropores while the decrease is due to the agglomeration of particles. Furthermore, T_γ^{max} rises with T_a. This result leads to conclude that the particle with higher annealing tempera-

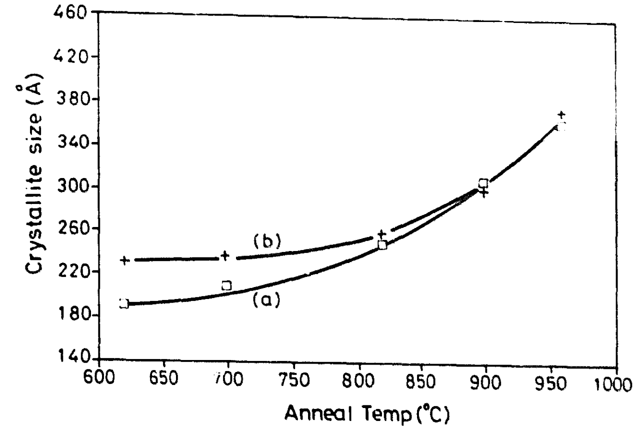

Fig. 4. Crystallite size (t) as a function of annealing temperature. (a) α-Fe_2O_3 particle, (b) resulting γ-Fe_2O_3 particle.

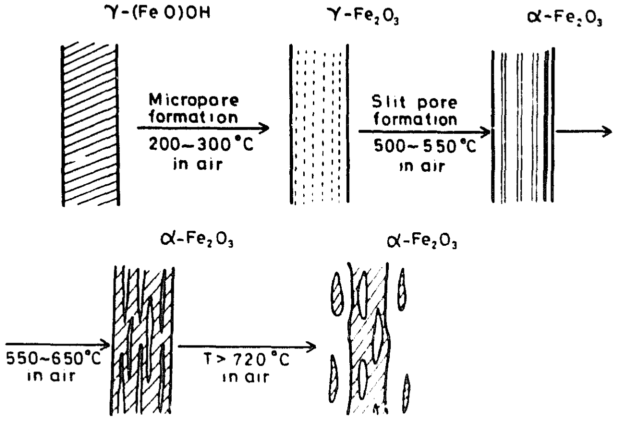

Fig. 5. Morphology variation of micropoles after various stages of heat treatments.

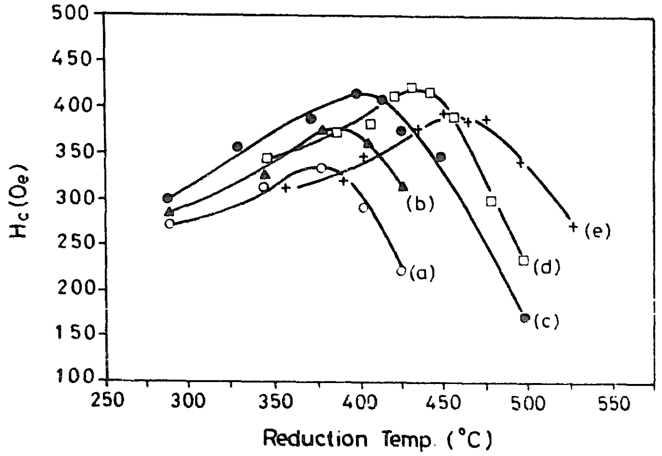

Fig. 6. Coercive force (H_c) of modified γ-Fe_2O_3 with 0.42 wt% Si as a function of reduction temperature (T_d). Oxidation temperature is 300 °C and oxidation time is 30 min. Annealing time is 1 h. (a) without annealing, (b) $T_a = 550\,°C$, (c) $T_a = 620\,°C$, (d) $T_a = 750\,°C$, (e) $T_a = 850\,°C$.

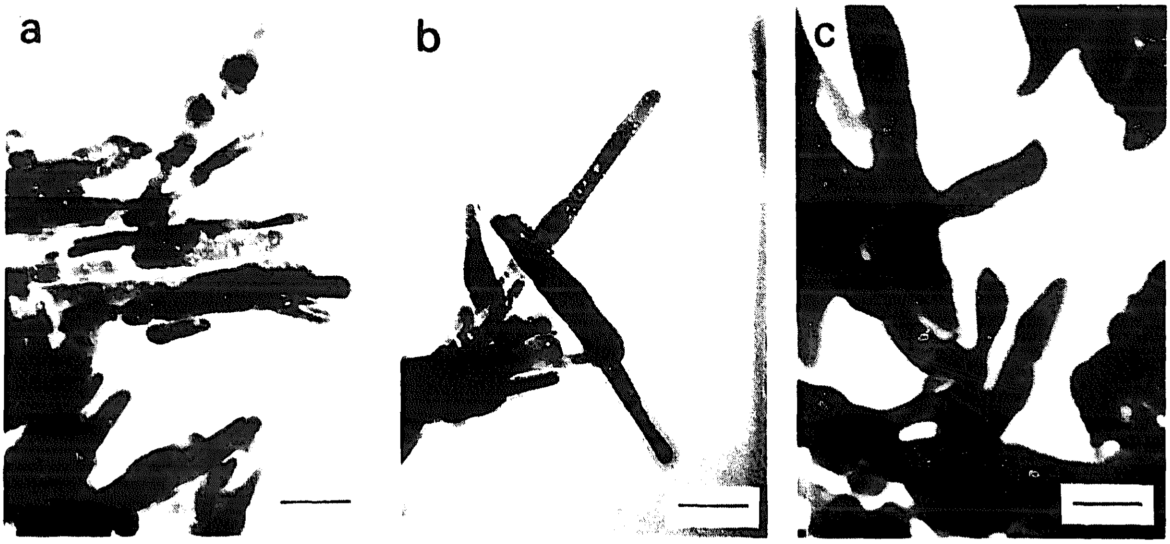

Fig. 7. Micrographs of modified γ-Fe_2O_3 with 0.42 wt% Si and no prior annealing. (a) $T_\gamma = 400\,°C$, (b) $T_\gamma = 440\,°C$, (c) $T_\gamma = 50\,°C$. Oxidation temperature is 300 °C and the oxidation time is 30 min.

ture also requires higher reduction temperature to complete the transformation from α-Fe_2o_3 to Fe_3O_4. As already shown, the crystallite grows larger with increasing T_a, thus increasing the path for diffusion of the Fe^{2+} ion. The reduction temperature has to be raised to promote the transformation from α-Fe_2O_3 to Fe_3O_4.

Compared without any prior annealing, the coercive force increases at least 100 Oe with adequate annealing. This fact can be manifested from fig. 7 that without any prior annealing treatment there are still many micropores inside the particle even though the reduction temperature is raised up to 440 °C. And we cannot further raise the reduction temperature without changing the acicular shape of the particles.

In fig. 8, the specific magnetic moment (σ_s) of γ-Fe_2O_3 is monotonically decreasing with Si content. The magnetic moment for 0.8 wt% Si modified γ-Fe_2O_3 is about 14% lower than that of the unmodified γ-Fe_2O_3. This drastic reduction in σ_s cannot be explained only by the addition of non-magnetic silica. Olson suggests that some reaction occurs on the surface during reduction [5]. Fayalite and hematite which are non-magnetic are formed simultaneously with reduction. Therefore, it is considered to be the main account for the large decrease of σ_s. It is also indicated in fig. 8 that H_c shows a maximum when Si content equals 0.42 wt%. It has been proved that the silica can inhibit the reduction [6]. Thus once the Si content exceeds 0.5 wt%, the reduction will not complete under these conditions and the particle will contain some α-Fe_2O_3 which are non-magnetic.

In the oxidation process from Fe_3o_4 to γ-Fe_2O_3, the intermediate state can be described as $Fe^{3+}[Fe^{3+}_{1+2x/3}Fe^{2+}_{1-x}\Delta_{x/3}]O_4$ where Δ is the vacancy and x is the degree of oxidation. The ratio of Fe^{2+}/Fe^{3+} is measured by chemical analysis. And from the ratio of Fe^{2+}/Fe^{3+}, the oxidation degree x can be found. The specific magnetic moment (σ_s) is plotted as a function of x for both

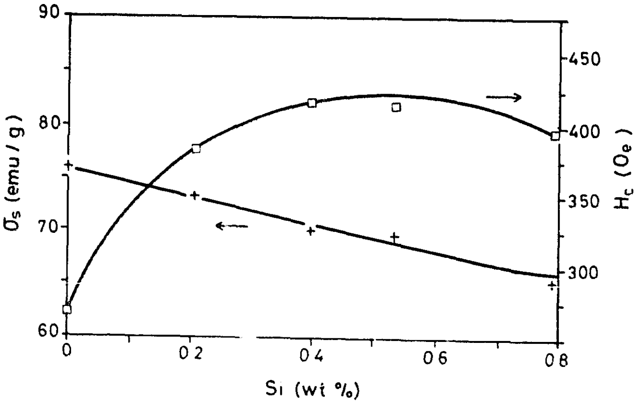

Fig. 8. Variation in coercive force and magnetization of Si-modified γ-Fe_2O_3 particles as a function of Si content. Reduction condition is 400 °C for 20 min and oxidation condition is 300 °C for 30 min.

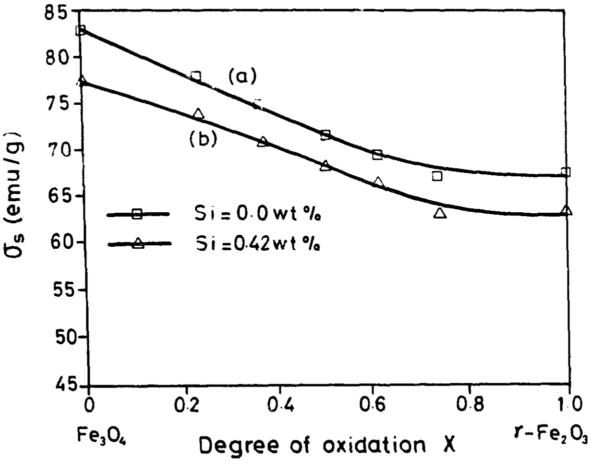

Fig. 9. Degree of oxidation dependence of specific magnetization (σ_s) for the unmodified and Si-modified particles.

unmodified and modified particles in fig. 9. Magnetic particles have a larger value of σ_s than maghemite particles so that σ_s should decrease with increasing x for both kinds. It is interesting to note in fig. 10 that for unmodified particles there is a peak in the coercive force at $x \approx 0.65$. If H_c is mainly originated from the shape anisotropy of the acicular particles, H_c should be proportional to the saturation magnetization and decrease with increasing x [7]. Thus some additional anisotropy has to be included to account for H_c. Borrelli suggested that Fe^{2+}-vacancy interaction be responsible for this behavior [8]. As to the Si-adsorbed particle, it exhibits a much different feature. H_c monotonically increases with x and the maximum enhancement of H_c is obtained for $x = 1$. It is then clear that in addition to the Fe^{2+}-vacancy interaction other mechanisms have to be considered.

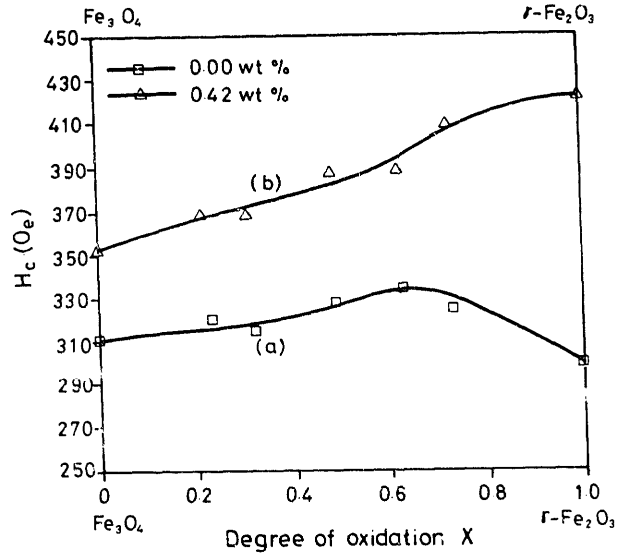

Fig. 10. Degree of oxidation dependence of coercive force (H_c) for the unmodified and Si-modified particles.

The effect of reduction of porosity due to the annealing is first considered. The Stoner–Wohlfarth model [7] is applied on a single-domain particle with several cavities [9]. The coherent magnetization reversal from unstable to stable state is implicit in this model. Only the interaction energy between the particles and micropores are taken into account and the magnetostatic energy among the micropores itself is neglected. From the superposition principle and the reciprocity theorem, the magnetic self-energy can be expressed as

$$E_m = \tfrac{1}{2}(\boldsymbol{M} \cdot \boldsymbol{D} \cdot \boldsymbol{M})\Big(v - \sum_i 2v^i\Big) + \tfrac{1}{2}\sum_i v^i(\boldsymbol{M} \cdot \boldsymbol{D}^i \cdot \boldsymbol{M}), \tag{2}$$

where $\boldsymbol{M}$ is the magnetization of the particle, $\boldsymbol{D}$ the demagnetization factor of the particle, v the volume of the particle, v^i and $\boldsymbol{D}^i$ the volume and demagnetization factor of each micropore, respectively. If the shape of micropores is a sphere, the second term in eq. (2) is only a constant. Therefore,

$$E_m = \tfrac{1}{2}(\boldsymbol{M} \cdot \boldsymbol{D} \cdot \boldsymbol{M})(v - 2v') \tag{3}$$

$$= \tfrac{1}{2}M_s^2(v - 2v')(N_\perp - N_\parallel)\sin^2\theta, \tag{4}$$

where v' is the total volume of micropores and M_s is the saturation magnetization. It implies that

$$H_c^p = (N_\perp - N_\parallel)M_s(1 - 2p), \tag{5}$$

where $p = v'/v$.

In our calculations, we assumed that the porosity is 20% before the heat treatment and 10% after the heat treatment. As shown in fig. 11, the reduction of the total volume of micropores will increase approximately the same amount of coercive force for different oxidation degree x (dashed line). Therefore, the monotonic increase of coercive force for silica-coated iron oxide particle with

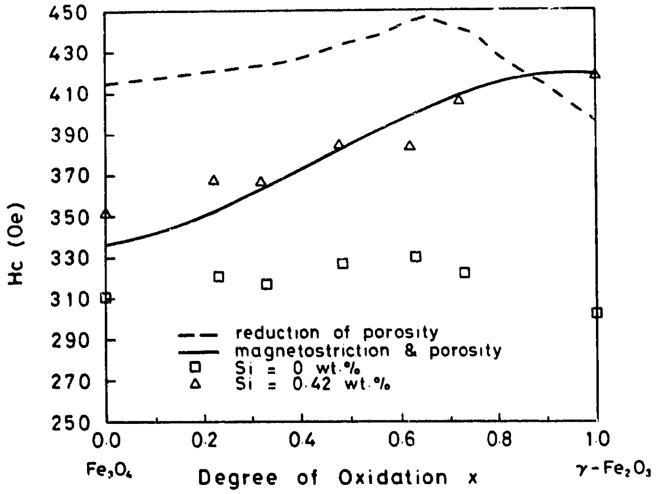

Fig. 11. Comparison of experimental data and theoretical results for coercive force.

x cannot be explained only by the reduction of micropores.

Olsen, using XPS, discovered the presence of Fe^{2+} ions near the surface of Si-modified γ-Fe_2O_3 particle [5]. Maeda et al. have also proved that this unusual increase in the coercive force requires the transformation process from Fe_3O_4 to γ-Fe_2O_3 [10]. Therefore, it leads to believe that a monolayer or less of fayalite is responsible for the enhancement of H_c. The magnetoelastic energy arises from the rather high stress between the lattice mismatch of fayalite and iron oxide change the coercive force in different ways. The lattice constant of Fe_2SiO_4, γ-Fe_2O_3 and Fe_3O_4 are taken as 8.234 [11], 8.33 and 8.40 Å [1], respectively. Furthermore, the lattice constant of the iron oxide particle with the oxidation degree x is taken as the linear interpolation of γ-Fe_2O_3 and Fe_3O_4 which is $8.40(1-x)+8.33x$ as shown in fig. 12. The magnetization M_s and magnetostriction constant λ_s are taken with a similar method, except that λ_s has one extra reference datum for the berthollide [1]. Therefore, the contribution of the coercive force to the magnetostriction can be determined, which is, $\Delta H_c = 3\lambda_s\sigma/M_s$. Because of the opposite influence of the magnetostriction effect on the magnetite and maghemite, the coercive force of silica-coated iron oxide will show different behavior (fig. 11). During the calculations, the Young's modulus of ferrite is taken as 3.0×10^{11} dyne/cm² [12]. The combination of porosity reduction and surface magnetoelastic effect can thus explain the anomolous increase in the coercive force for silica-adsorbed iron oxide particle of different oxidation degree. The results of this calculation also suggests that the neutralization of "easy" reversal sites, or the reduction of spin canting at the particle's surface is not responsible for the increase of coercive force of non-magnetic coated iron oxide particle [13].

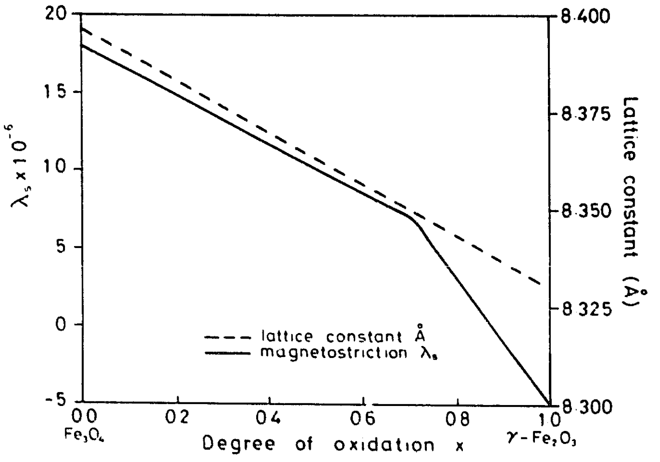

Fig. 12. Relationship of lattice constant and magnetostriction with degree of oxidation x.

References

[1] E.P. Wohlfarth, ed., Ferromagnetic Materials, vol. 2 (North-Holland, Amsterdam, 1980) chap. 7.

[2] P.E. Eagle and J.C. Mallinson, J. Appl. Phys. 38 (1976) 995.

[3] H. Morita et al., US Pat. 173 618 (30 July 1980).

[4] A. Cullity, Elements of X-ray diffraction, 2nd ed. (Addison-Wesley, New York, 1978) p. 102.

[5] K.H. Olsen, J. Magn. Magn. Mat. 54–57 (1986) 1691.

[6] A.R. Corradi and E. Melloceresa, IEEE Trans. Magn. MAG-15 (1979) 1068.

[7] E.C. Stoner and E.P. Wohlfarth, Phil. Trans. Roy. Soc. (London) A 240 (1948) 599.

[8] N.F. Borrolli, S.L. Chen and J.A. Murphy, IEEE Trans. Magn. MAG-8 (1972) 648.

[9] W.F. Brown, Jr. and A.H. Morrish, Phys. Rev. 105 (1957) 1198.

[10] Y. Maeda et al., Proc. Intern. Conf. Ferrites, Japan (Sept.–Oct. 1980) p. 541.

[11] F. Marumo and Isobe, Acta Crystallogr. Sect. B 33 (1977) 713.

[12] J. Smit and H.P.J. Wijn, Ferrites (John Wiley, New York, 1959) p. 225.

[13] A.E. Berkowitz, IEEE Trans. Magn. MAG-22 (1986) 466.